darkness alone could have brought about the Cretaceous-Tertiary boundary extinction event only if its duration was greater than 3 to 5 months or if the dinosaurs were occupying high latitudes only during part of the year, which may be unlikely for some of the small, large-eyed, large-brained Victorian hypsilophodontids.

REFERENCES AND NOTES

1. A. S. Woodward, *Annu. Mag. Nat. Hist.* 7, 1 (1906).
2. R. E. Molnar, T. F. Flannery, T. H. V. Rich, *Alcheringa* **5**, 141 (1981); S. P. Welles, *J. Paleontol.* **57**, 196 (1983); R. E. Molnar, T. F. Flannery, T. H. V. Rich, *ibid.* **59**, 1511 (1985).
3. E. M. Brouwers *et al.*, *Science* **237**, 1608 (1987); J. M. Parrish, J. T. Parris, J. H. Hutchison, R. A. Spicer, *Palaios* **2**, 377 (1987); K. L. Davies, *J. Paleontol.* **61**, 198 (1987); L. J. Bryant, *Paleobios* **40**, 1 (1983); D. A. Russell, *Syllogeus* **53**, 1 (1984).
4. R. T. Gregory, C. B. Douthitt, I. R. Duddy, P. V. Rich, T. H. Rich, *Earth Planet. Sci. Lett.*, in press.
5. J. W. Warren, *Mem. Natl. Mus. Victoria, Melbourne* **29**, 23 (1969).
6. R. E. Molnar, *Mem. Soc. Geol. Fr.* **NS 59**, 131 (1980).
7. J. A. Talent, P. M. Duncan, P. L. Hanby, *Emu* **66**, 81 (1966).
8. M. Waldman, *Spec. Pap. Palaeontol.* **9**, 1 (1971).
9. B. J. J. Embleton and M. W. McElhinny, *Earth Planet. Sci. Lett.* **58**, 141 (1982); M. Idnurm, *Geophys. J. R. Astron. Soc.* **83**, 399 (1985).
10. M. E. Dettmann, *Proc. R. Soc. Victoria* 77, 1 (1963); M. E. Dettmann, *Assoc. Australas. Palaeontol. Mem.* **3**, 79 (1986); B. E. Wagstaff and J. R. E. McEwen Mason, *Nat. Geog. Res.*, in press.
11. A. N. Drinnan and T. C. Chambers, *Assoc. Australas. Palaeontol. Mem.* **3**, 1 (1986).
12. J. G. Douglas *et al.*, *Spec. Publ. Geol. Soc. Aust.* **5**, 143 (1976). J. J. Veevers, *Earth Planet. Sci. Lett.* 77, 91 (1986); S. C. Cande and J. C. Mutter, *ibid.* **58**, 151 (1982); J. J. Veevers and S. L. Eittreim, *Aust. J. Earth Sci.* **35**, 355 (1988).
13. B. E. Wagstaff, thesis, Monash University, Melbourne (1983); E. D. Gill, *Proc. R. Soc. Victoria* **89**, 7 (1977); G. A. Lees and R. A. F. Cas, unpublished data; I. R. Duddy, thesis, Melbourne University (1983).
14. A. J. W. Gleadow and I. R. Duddy, *Proceedings of the Fifth International Gondwana Symposium, Wellington, New Zealand* (Balkema, Rotterdam, 1980), p. 295.
15. N. M. Lindsay, thesis, University of Melbourne (1982).
16. T. H. Rich and P. V. Rich, in preparation.

16a. R. Jupp and A. A. Warren, *Alcheringa* **10**, 99 (1986).

17. P. A. Jell and P. M. Duncan, *Assoc. Australas. Palaeontol. Mem.* **3**, 111 (1986).
18. E. S. Gaffney, personal communication.
19. D. Rogers, thesis, Monash University, Melbourne (1987).
20. J. G. Douglas and G. E. Williams, *Palaeogeogr. Palaeoclimatol. Palaeoecol.* **39**, 171 (1982); ——— and J. G. Douglas, *ibid.* **49**, 355 (1985).
21. H. J. Jerison, *Evolution of the Brain and Intelligence* (Academic Press, New York, 1973). The parameter *EQ* is the ratio of actual brain size to expected brain size.
22. J. A. Hopson, *Annu. Rev. Ecol. Syst.* **8**, 429 (1979).
23. D. A. Russell, *Can. J. Earth Sci.* **6**, 595 (1969).
24. E. T. Gill, E. R. Segnit, N. H. McNeill, *Proc. R. Soc. Victoria* **89**, 51 (1977).
25. T. E. Cerling, *Earth Planet. Sci. Lett.* **71**, 229 (1984).
26. J. R. Gat, in *Handbook of Environmental Isotope Geochemistry*, P. Fritz and J. Ch. Fontes, Eds. (Elsevier, New York, 1980), vol. 1, p. 21.
27. S. Joussaume, R. Sadourny, J. Jousel, *Nature* **311**, 24 (1984).
28. L. A. Frakes and J. E. Francis, *ibid.* **333**, 547 (1988).
29. J. C. Vogel, J. C. Lerman, W. G. Mook, *Hydrol. Sci. Bull.* **20**, 203 (1975); H. Bouwer, *Groundwater Hydrology* (McGraw-Hill, New York, 1978).
30. W. Dansguard, *Tellus* **16**, 436 (1964).
31. L. A. Frakes *et al.*, *Palaeogeogr. Palaeoclimatol. Palaeoecol.* **59**, 31 (1987).

32. We thank Atlas Copco, the National Geographic Society, the Australian Research Grants Scheme, David Holdings Ltd., Mobil Oil, Imperial Chemical Industries, J. Herman, W. Loads, J. Chessells, the Friends and Council of the Museum of Victoria, and the Sunshine Foundation for supporting this research; L. Kool for preparing much of the material; and D. Gelt, S. Morton, F. Coffa, P. Hermansen, and S. Fay for graphics, photography, and manuscript preparation. The isotopic analyses were made possible through the support from the Australian Research Council, National Energy Research, Development and Demonstration Council, and Esso Australia. I. Duddy kindly allowed access to his extensive concretion collection and his sedimentological analysis of the Otway Group.

3 June 1988; accepted 13 September 1988

X-ray Scattering Studies of Aligned, Stacked Surfactant Membranes

ERIC B. SIROTA, GREGORY S. SMITH,* CYRUS R. SAFINYA, ROBERT J. PLANO, NOEL A. CLARK

X-ray scattering studies were performed to understand the structure and correlations in the lamellar phases of thick, freely suspended films of (i) the hydrated phospholipid dimyristoylphosphotidylcholine (DMPC) and (ii) the ternary system consisting of the surfactant sodium dodecyl sulfate (SDS), cosurfactant (pentanol), and water. The films were drawn in a temperature- and humidity-controlled environment, where the layers were oriented to within 0.1°. In the DMPC system, this made it possible to directly observe the orientation of the $P_{\beta'}$ modulation and to identify phase $L_{\beta'}$ as three distinct phases distinguished by the direction of chain tilt with respect to the lattice. In the L_α phase of the ternary system, power law behavior of the (0,0,L) structure factor arising from the algebraic decay of layer correlations was observed in single crystals.

SINCE THE LIPID MOSAIC MODEL OF cell membranes was proposed (*1*), much work has been done to understand the details of their function and structure. Although actual cell membranes consist of many components including lipids, cholesterol, and proteins, a great deal can be learned from the study of simple model systems that contain either a subset of those components or components similar to those found in real membranes. These are lyotropic, liquid crystalline phases (*2–5*), which are also of scientific interest because they are prototype models for elucidating the nature of phases and their transitions in two-dimensional (2D) systems. Furthermore, because of their ability to buckle out of their 2D plane, these phases provide real models for studies of the statistical physics of crumpled surfaces imbedded in three-dimensional (3D) space (*6*).

The high-water-content portion of the phase diagram of phospholipids was known to consist of three lamellar regions. The L_α phase, characterized by disordered chains and a lack of positional order within the layer, has been the subject of a great deal of study (*2–5*) because surfactants in most living membranes are in this state. The $P_{\beta'}$ phase is of particular interest as a result of the presence of a long wavelength (80 Å $< \lambda <$ 120 Å) modulation of the layers. The $L_{\beta'}$ phase was believed to have tilted molecules and, although occupying a large portion of the phase diagram, it was largely ignored. We have expanded on a technique (*7*) by which we can produce extremely well-aligned, freely suspended films of the samples in continuously variable humidity con-

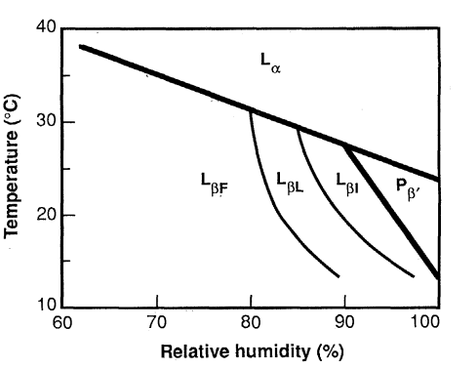

Fig. 1. The temperature-humidity phase diagram of DMPC. Because both axes are related to thermodynamic potentials, there are no two-phase regions. Note that the phase previously known as $L_{\beta'}$ is, in fact, three distinct phases, $L_{\beta F}$, $L_{\beta L}$, and $L_{\beta I}$.

E. B. Sirota, C. R. Safinya, R. J. Plano, Exxon Research and Engineering Company, Corporate Research Science Laboratories, Route 22 East, Annandale, NJ 08801.
G. S. Smith, Exxon Research and Engineering Company, Corporate Research Science Laboratories, Route 22 East Annandale, NJ 08801, and Department of Physics, University of Colorado, Boulder, CO 80309.
N. A. Clark, Department of Physics, University of Colorado, Boulder, CO 80309.

*Present address: Los Alamos Neutron Scattering Center, Los Alamos National Laboratory, Los Alamos, NM 87545.

ditions (*5*), which allows us to gain information previously not available without the alignment. This technique has been of great utility in studying thermotropic (dry) liquid crystals and the physics of 2D systems (*7–9*). In this report, we show its importance in the study of biologically relevant systems.

The phospholipid chosen for study was DMPC (*10*). We were able to produce freely suspended films of hydrated lipids in a controlled humidity environment (≥400 bilayers thick). By smearing hydrated L_α sample across a hole (5 mm in diameter) in a thin plate, the lamellae in the film oriented to within 0.1° of the surface normal. Because these systems often form weakly ordered structures where only a few scattering peaks are observed, such a high degree of orientation is essential for determining many structural properties of these phases. The films were drawn and the measurements performed in a chamber where the temperature (T) was controlled by means of thermoelectric devices and the relative humidity (RH) was controlled to ±0.2% by means of a gas flow system (*5*) with dew point–sensing hygrometers for feedback and reading. By varying the humidity, which is directly related to the chemical potential of water [$\Delta\mu = RT \ln(RH/100)$, where R is the gas constant], we can continuously vary the amount of water in the layers.

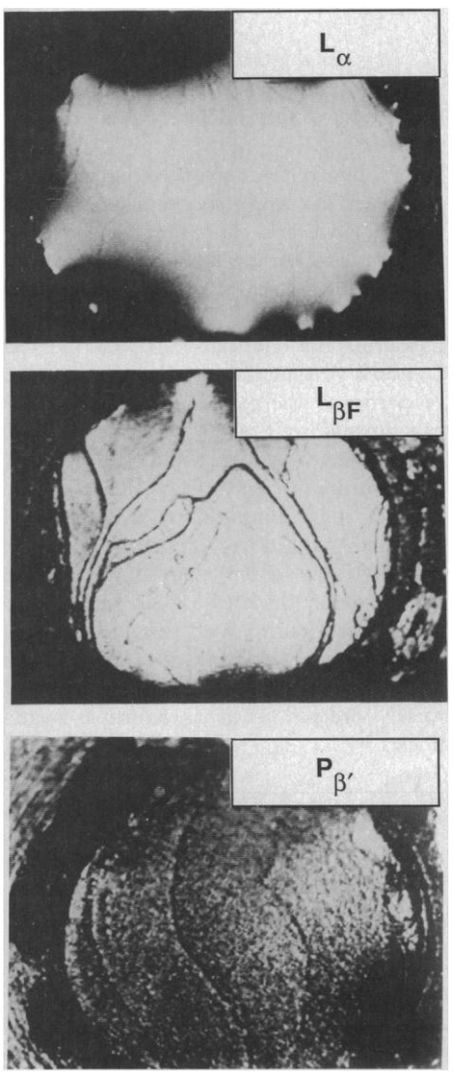

Fig. 2. Photographs of thick, freely suspended hydrated DMPC films observed in reflected white light in the L_α, $L_{\beta F}$, and $P_{\beta'}$ phases. The three $L_{\beta'}$ phases are optically indistinguishable.

The phase diagram (Fig. 1) was mapped out reproducibly as a function of T and RH. Because RH is effectively a thermodynamic potential, there are no two-phase regions in this phase diagram, such as one obtains with gravitometrically prepared samples (*4*). The films in these three phases have characteristic textures when viewed with reflected white light (Fig. 2), which helped in mapping out the phase diagram. The L_α phase appears very smooth and shiny. The three $L_{\beta'}$ phases, indistinguishable optically, appeared rougher. The $P_{\beta'}$ phase appears grainy in texture.

The scattering studies were done on Huber four-circle diffractometers with an 18-kW Rigaku rotating anode x-ray generator at Exxon, and also with synchrotron radiation at the Stanford Synchrotron Radiation Laboratory beam-line 7-2 and the National Synchrotron Light Source (Brookhaven) Exxon beam-line X10A. The sample cell was designed to allow both scattering in transmission to study the in-plane structure and reflection from the surface of the film to measure the bilayer repeat distance (d) as well as the nature and magnitude of layer undulations.

We were able to directly observe in the $P_{\beta'}$ phase the orientation of the modulation wave vector, on a freely suspended aligned sample. The sample was about 2 μm thick (~400 bilayers), and the layer normals were aligned to better than 1°. The modulation, measured at $T = 20.6$°C and 94% RH where $d = 55.9$ Å, was shown to have a wave vector of magnitude $q = 0.035 \pm 0.002$ Å^{-1} ($\lambda = 180$ Å) tilted 7.5° out of the plane of the layers. This is consistent with interpretations of powder diffraction data (*11*). Figure 3A shows a scan in reciprocal space along the direction of the modulation where four orders of reflections are visible. Because of the orientational quality of our samples and the use of a high-resolution x-ray spectrometer at the synchrotron facilities, we were able to obtain unique information on the structural nature of the modulation. The anharmonic nature of the modulation is evident, consistent with freeze-fracture direct image data (*12*), by the appearance of strong higher harmonics of the modulation.

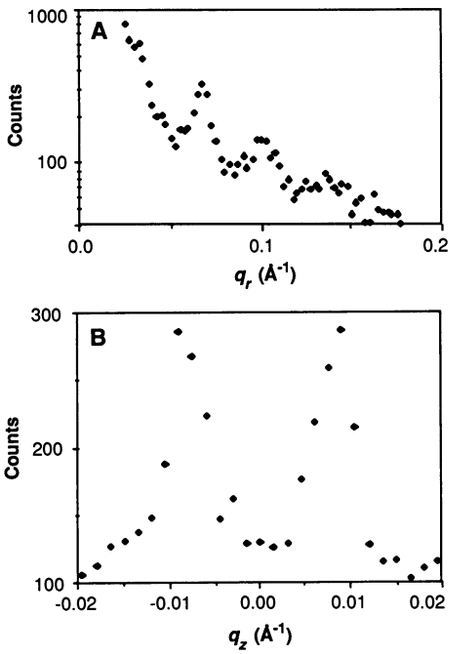

Fig. 3. (**A**) X-ray data from a scan along a line in reciprocal space tilted 7.5° out of the plane of the layers, showing four orders of the reflection of the modulation wave vector ($q = 0.035$ Å^{-1}) in the $P_{\beta'}$ phase at 94% RH, $T = 20.6$°C. (**B**) Scan through the second harmonic, normal to the plane of the layers at $q_r = 0.069$ Å^{-1}, where the splitting of the peaks off axis shows the orientation of the modulation directly. (Rocking scans at this wave vector were used to verify the orientation.) Although the layer normals are well aligned, there is no alignment within the layer, so the scattering is cylindrically averaged giving peaks at both $+q_z$ and $-q_z$.

Figure 3B shows a q_z scan (normal to the layers) through the second harmonic of the modulation (at $q_r = 0.069$ Å^{-1}). The peak width, limited by the sample mosaic, set a lower limit on the coherence of the modulation of at least 1000 Å. Although there is no evidence that the in-plane positional order of the molecules is correlated across the water layers, the long wavelength modulation is three dimensionally ordered.

In the $L_{\beta'}$ region, instead of finding one phase, as was expected, we found three distinct phases that we have labeled $L_{\beta F}$, $L_{\beta L}$, and $L_{\beta I}$ (the subscripts coming from thermotropic liquid crystal nomenclature [see (*8*) and references therein]. The average tilts of the chains in these phases, as determined from the scattering, is shown in Fig. 4 (top). In all three phases the in-plane positional order extends ~200 Å and is not correlated across water layers. The magnitude of the chain tilt increases continuously with increasing RH from ~26° in $L_{\beta F}$ to 30° in $L_{\beta I}$. The phases are distinguished by the direction of the tilt with respect to the local distorted hexagonal lattice. In $L_{\beta F}$, the tilt is between nearest neighbors; in $L_{\beta I}$, it is

toward a nearest neighbor; and in $L_{\beta L}$, it varies continuously between the two, with second-order transitions on both ends. These phases are distinct by symmetry. The details of the scattering and the relation between real and reciprocal space structures are discussed elsewhere (*13*). In addition to the fact that $L_{\beta'}$ must now be distinguished by a subscript, it is also clear that a high degree of orientation of the layers is necessary to identify these phases. Schematics of the scattering in reciprocal space are shown in Fig. 4 (bottom). As one can see, poor alignment of the layer normal would cause the patterns to be smeared out along the curved line, causing the distinctions between the phases to be lost; thus, they remained undetected until now.

Oriented films in the L_α phase allow us to directly measure the magnitude of undulations of the bilayer membranes, which gives us information relating to the bending modulus of a bilayer (k_c) and the bulk compressibility of the bilayers (B) in that medium. Peierls (*14*) and Landau (*15*) were the first to recognize that 3D structures that are periodic in only one direction, such as the lyotropic L_α phase, are marginally stable to thermal fluctuations that destroy the long-range order and change the δ-function (0,0,L) peaks from the layers to less sharp algebraic singularities whose form is asymptotically (*16*)

$$S(0,0,q_z) = (q_z - q_m)^{\eta_m - 2} \qquad (1)$$

where

$$\eta_m = \frac{\pi m^2 k_b T}{2d^2(Bk_c/d)^{1/2}} \qquad (2)$$

(k_b is the Boltzmann constant) near the peak positions ($q_m = 2\pi m/d$, where m is an integer). This power law behavior for the first harmonic ($m = 1$) of $S(q)$ has been confirmed in a thermotropic smectic-A system (*17*). More recently, the power law behavior and the scaling of η_m with m^2 has been confirmed for the first two harmonics of $S(q)$ in a series of quaternary and ternary systems in the lyotropic L_α phases in randomly oriented samples (*3*).

Although the mean-square height variation of a bilayer diverges with the size of the sample, it does so only logarithmically and is given by (*15, 16*)

$$\langle u^2 \rangle = \frac{d^2 \eta_1 \ln(L/a)}{2\pi^2} \qquad (3)$$

where L is the characteristic length over which the average is taken, and a is the in-plane interparticle distance. Using the full (nonasymptotic forms) of $S(q)$, we can also determine k_c and B independently (*3*).

Scattering data from the first two harmonics in freely suspended films of the ternary system SDS, pentanol, and water in a sealed cell with the film in equilibrium with the vapor phase of the mixture are contrasted with data from the DMPC-water system in Fig. 5. In the ternary system, pentanol reduces the bending modulus, increasing undulations (*18*) and giving $\eta_1 = 0.23 \pm 0.03$ as determined by the statistical errors of a least-squares fit. For the pure DMPC system, the layers are much stiffer, so $\eta_1 = \eta_6/36 < 0.003$. From these results we can estimate $\langle u^2 \rangle / d^2 = 0.09$ for SDS-pentanol-water and <0.001 for DMPC (averaged over 1 μm). With this technique, the effect of various cosurfactants on the elastic properties of membranes can be directly probed.

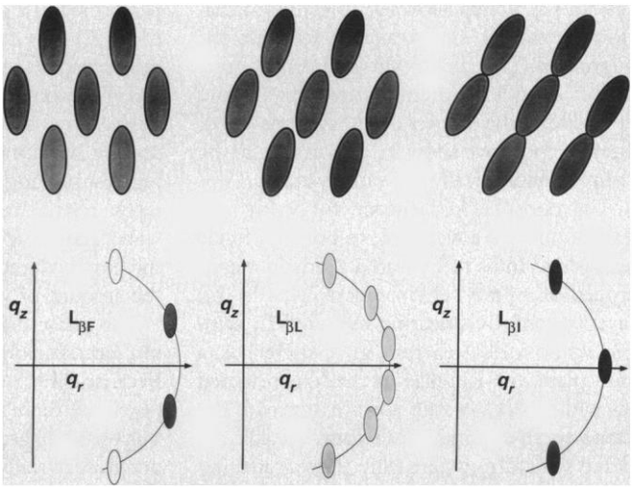

Fig. 4. (**Top**) Schematic showing the relation between the tilt direction and the lattice positions of chains in $L_{\beta F}$ (left), $L_{\beta L}$ (center), and $L_{\beta I}$ (right). The sketch is a view (only of the chains) looking down on the layers, so the chains appear elongated in the direction of tilt. (**Bottom**) Schematic of the measured scattering from these three phases; q_z is normal to the layers and q_r is in the plane of the layers. The sample's normal is well oriented, but the scattering is cylindrically averaged. The darker spots represent scattering approximately twice as strong as the lighter spots. The width of the peaks along q_z is determined by the length of the chains in a bilayer, as there is no molecular positional correlation across water layers in any of these phases. The peak width along q_r corresponds to correlated regions that are ~200 Å in diameter. Misorientation of the layer normal would smear out the peaks along the curved line, making the three phases indistinguishable. Actual (q_r, q_z) coordinates of the peaks are as follows (in $Å^{-1}$): $L_{\beta F}$ (1.446 ± 0.35) and (1.350 ± 0.70); $L_{\beta L}$ (1.355 ± 0.64), (1.399 ± 0.52), and (1.468 ± 0.15); $L_{\beta I}$ (1.365 ± 0.65) and (1.475 ± 0.0).

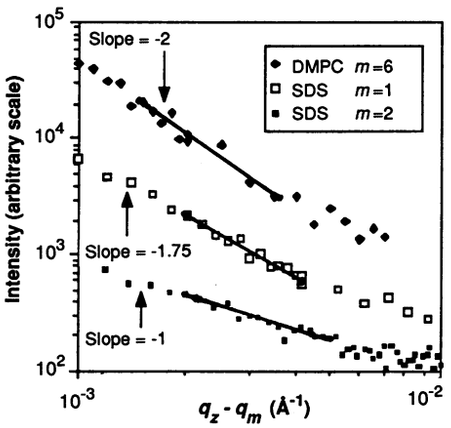

Fig. 5. Log-log plot of the scattering intensity from the tails of the first and second harmonics of the ternary mixture [SDS (30% by weight), pentanol (23%), water (47%)] and the sixth harmonic of DMPC-water (90% RH, 31°C). From the low q slopes, one determines that for the SDS system $\eta_1 = 0.23$ whereas for DMPC $\eta_1 < 0.003$.

In summary, we have demonstrated the power of the freely suspended film technique for lyotropic multimembrane systems by directly measuring the modulation orientation in the $P_{\beta'}$ phase; by distinguishing the three $L_{\beta'}$ phases ($L_{\beta F}$, $L_{\beta L}$, and $L_{\beta I}$); and by measuring the line shapes of well-oriented L_α peaks, yielding information on the elastic properties of the membranes. The DMPC experiments were done under controlled and continuously variable humidity. It is also possible to control the thickness of these films from hundreds of molecular layers down to a single bilayer in order to determine the effects due to the surface layers or finite thickness (*8*). In general, the alignment obtained with this technique is useful, if not essential, in measuring structure and correlations in systems that are weakly ordered, such as lyotropic membranes.

REFERENCES AND NOTES

1. S. J. Singer and G. L. Nicolson, *Science* **175**, 720 (1972).
2. For a review see P. S. Pershan, *Phys. Today* **35**, 34 (May 1982).
3. C. R. Safinya *et al.*, *Phys. Rev. Lett.* **57**, 2718 (1986); D. Roux and C. R. Safinya, *J. Phys. (Paris)* **49**, 307 (1988).
4. M. J. Janiak, D. M. Small, G. G. Shipley, *J. Biol. Chem.* **254**, 6068 (1979); A. Tardieu, V. Luzzatti, F. C. Reman, *J. Mol. Biol.* **75**, 711 (1973); V. A. Parsegian, N. Fuller, R. P. Rand, *Proc. Natl. Acad. Sci. U.S.A.* **76**, 2750 (1979); G. L. Kirk, S. M. Gruner, D. L. Stein, *Biochemistry* **23**, 1093 (1984); M. B. Schneider and W. W. Webb, *J. Phys. (Paris)* **45**, 273 (1984).
5. G. S. Smith, C. R. Safinya, D. Roux, N. A. Clark, *Mol. Cryst. Liq. Cryst.* **144**, 235 (1987).

6. D. R. Nelson and L. Peliti, *J. Phys. (Paris)* **48**, 1095 (1987); J. A. Aronovitz and T. C. Lubensky, *Phys. Rev. Lett.* **60**, 2634 (1988).
7. C. Y. Young, R. Pindak, N. A. Clark, R. B. Meyer, *Phys. Rev. Lett.* **40**, 773 (1978); D. E. Moncton and R. Pindak, *ibid.* **43**, 701 (1979).
8. E. B. Sirota, P. S. Pershan, L. B. Sorensen, J. Collett, *Phys. Rev. A* **36**, 2890 (1987).
9. J. D. Brock *et al.*, *Phys. Rev. Lett.* **57**, 98 (1986).
10. DMPC, >99% pure, obtained from Avanti Polar Lipids, Birmingham, AL.
11. D. Wack and W. W. Webb, *Phys. Rev. Lett.* **61**, 1210 (1988).
12. J. A. N. Zasadzinski, J. Schneir, J. Gurley, V. Elings, P. K. Hansma, *Science* **239**, 1013 (1988).
13. G. S. Smith, E. B. Sirota, C. R. Safinya, N. A. Clark, *Phys. Rev. Lett.* **60**, 813 (1988).
14. R. E. Peierls, *Helv. Phys. Acta Suppl.* 7, 81 (1934).
15. L. D. Landau, in *Collected Papers of L. D. Landau*, D. Ter Haar, Ed. (Gordon & Breach, New York, 1965), p. 209.
16. A. Caille, *C. R. Acad. Sci. Ser. B* **274**, 891 (1972).
17. J. Als-Nielsen *et al.*, *Phys. Rev. B* **22**, 312 (1980).
18. C. R. Safinya, E. B. Sirota, D. Roux, G. S. Smith, in preparation.
19. We acknowledge helpful conversations with D. Roux and S. K. Sinha and the technical assistance of R. Hewitt, M. Sansone, and K. D'Amico. Part of this work was done at the Stanford Synchrotron Radiation Laboratory and at the National Synchrotron Light Source (Brookhaven), which are funded by the Department of Energy. Part of this research was supported by joint Industry-University NSF grant DMR-8307157.

7 July 1988; accepted 30 September 1988

Neonatal Hepatitis Induced by α_1-Antitrypsin: A Transgenic Mouse Model

MARK J. DYCAICO, SETH G. N. GRANT, KATHERINE FELTS, W. STEPHEN NICHOLS, STEPHEN A. GELLER, JEFFREY H. HAGER, AMY J. POLLARD, STEVEN W. KOHLER, HEIDI P. SHORT, FRANK R. JIRIK, DOUGLAS HANAHAN, JOSEPH A. SORGE*

Transgenic mouse lineages were established that carry the normal (M) or mutant (Z) alleles of the human α_1-antitrypsin (α_1-Pi) gene. All of the α_1-Pi transgenic mice expressed the human protein in the liver, cartilage, gut, kidneys, lymphoid macrophages, and thymus. The human M-allele protein was secreted normally into the serum. However, the human Z-allele protein accumulated in several cell types, but particularly in hepatocytes, and was found in serum in tenfold lower concentrations than the M-allele protein. Mice in one lineage carrying the mutant Z allele expressed high levels of human α_1-Pi RNA and displayed significant runting (50% of normal weight) in the neonatal period. This lineage was found to have α_1-Pi–induced liver pathology in the neonatal period, concomitant with the accumulation of human Z protein in diastase-resistant cytoplasmic globules that could be revealed in the Periodic acid–Schiff reaction (PAS). The phenotype of mice in the strain expressing high levels of the Z allele is remarkably similar to human neonatal hepatitis, and this strain may prove to be a useful animal model for studying this disease.

THE α_1-PROTEASE INHIBITOR (α_1-antitrypsin; α_1-Pi) is a serum protein that inhibits trypsin, elastase, thrombin, chymotrypsin, factors XI and XIII, and plasmin. Its major physiologic function is to inhibit neutrophil elastase, providing 90% of the antielastase activity of serum (*1*). Individuals with α_1-Pi deficiency are at an increased risk of developing emphysema, usually in the fourth to fifth decades of life. The lung pathology results from the destruction of alveolar walls, presumably because of the unchecked activity of neutrophil elastase.

Genetically, α_1-Pi deficiency is autosomal and expressed in a codominant pattern. Approximately 100,000 individuals in the United States have clinical α_1-Pi deficiency. The most common alleles of the gene are designated as Pi^M (normal, with a gene frequency of 0.95), Pi^S (0.03), and Pi^Z (0.02). The MM, ZZ, and MZ phenotypes are associated with serum α_1-Pi levels of 2, 0.3, and 1.2 mg/ml, respectively.

The protein itself has a molecular size of 53 kD with three or four carbohydrate side chains. Its major site of synthesis is the liver. The S mutant contains a valine instead of a glutamic acid at amino acid position 264. The Z mutant contains a lysine instead of a glutamic acid at position 342 (*2, 3*). The Z mutation does not affect the amount of protein synthesized by the liver nor the ability of the protein to inhibit proteases, but rather affects the transport of the protein across the rough endoplasmic reticulum of liver cells. Liver histology of ZZ patients typically reveals diastase-resistant PAS-positive globules in the periportal hepatocytes (*4*), reflecting the buildup of the protein as a result of the transport defect. The transport mechanism in the endoplasmic reticulum is not known.

Approximately 15% of neonates with the ZZ genotype develop hepatitis; 25% of these develop obstructive jaundice and cirrhosis, and eventually die before age 8 (*5*). The pathophysiology has been attributed to intracytoplasmic inclusions of α_1-Pi within hepatocytes (*6*). It is suspected that neonates with hepatitis are more likely to develop cirrhosis as adults. It is not known why only 15% of ZZ homozygotes develop hepatitis, although it has been suggested that increased liver damage in these individuals is caused by expression of higher levels of protein in liver cells. It is also not known why boys develop α_1-Pi hepatitis more often than girls by a 2:1 ratio. In adults, liver disease associated with α_1-Pi is seen primarily in the form of cirrhosis. About 17% of all adults with nonalcoholic cirrhosis have the MZ heterozygous genotype (*7*). Again, there is a 2:1 ratio of male to female α_1-Pi patients with nonalcoholic cirrhosis.

To study the effects of human α_1-Pi alleles, transgenic mice were produced that contain the human α_1-Pi M and Z genes. To increase the probability of regulated, high-level expression, genomic λ clones that contained a substantial amount of 5′ flanking region were isolated (Fig. 1). A Sna B1–Eco RI fragment (6.1 kb) of the λ clone containing the M allele was exchanged with the same length fragment from a clone containing the Z mutation located in exon G (Fig. 1). Thus two clones, each containing 21.4 kb of human α_1-Pi sequence, were produced that differed at a single nucleotide responsible for the Z mutation. The presence of the Z mutation was confirmed by nucleotide sequencing.

The 21.4-kb Sal I fragments were gel purified and injected into fertilized F2 mouse embryos derived by intercrossing B6D2F1/J (C57BL/6J × DBA/2J) mice (*8*).

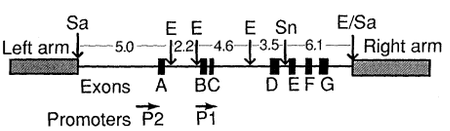

Fig. 1. Map of the human α_1-Pi genomic clone used to construct transgenic animals. Exons A and B and the macrophage-specific promoter (P_2) have recently been discovered (*17*); exon C was originally referred to as exon 1. P_1 is the hepatocyte-specific promoter. The distances between restriction sites are in kilobases. Genomic libraries were constructed in λ EMBL-3 from normal human DNA and from cell line GM3578, which is homozygous for the α_1-Pi Z allele. E, Eco RI, Sa, Sal I, Sn, Sna BI.

M. J. Dycaico, K. Felts, A. J. Pollard, S. W. Kohler, H. P. Short, F. R. Jirik, J. A. Sorge, Stratagene, La Jolla, CA 92037.
S. G. N. Grant, J. H. Hager, D. Hanahan, Cold Spring Harbor Laboratories, Cold Spring Harbor, NY 11724.
W. S. Nichols and S. Geller, Department of Pathology and Laboratory Medicine, Cedars Sinai Medical Center, Los Angeles, CA 90048.

*To whom correspondence should be addressed.